IOSR Journal of Mechanical and Civil Engineering (IOSR-JMCE)
e-ISSN: 2278-1684,p-ISSN: 2320-334X, Volume 18, Issue 5 Ser. I (Sep. – Oct. 2021), PP 17-21
www.iosrjournals.org

Performance analysis of Integrated solar combined cycle in the southern state of India

Pavankumar Deshmukh[1] Dr. Praveen kumar[2]
[1]*Department of Mechanical Engineering, Dayananda Sagar college of Engineering, Bengaluru-560078, INDIA*
[2]*Department of Mechanical Engineering, P.D.A College of Engineering Kalaburgi-585101,INDIA*

Abstract: *The Integrated Solar Combined Cyclesnow a day themostefficientsystemforconvertingsolarenergyintoelectricityamongallthehybridsolarthermaltechnologiesavailable. A parabolic trough solar field is coupled with a conventional combined cycle in this power plant. The performance ofanISCCplantunder southern state of Indiahasbeeninvestigatedinthisarticle. To that end, a thermodynamic model has been created to assess the intensity of solar radiation as well as the overall performance of the hybrid solar power plant.During bright periods, solar to power efficiency could reach 15.4 percent, according to the study. Furthermore, a 60 percent overall thermal efficiency is possible. Several operation characteristics, including as the time of day, the mass flow rate of the heat transfer fluid, and the angle of incidence on the collector surface, have also been discovered to improve the quantity of electricity produced.*

Keywords: *ISCC, DNI, GSR, WSR, HRSG, HSSG*

Date of Submission: 25-08-2021 Date of Acceptance: 09-09-2021

I. Introduction

Parabolic trough technology has been used for power production and mechanical driving applications since 1913. This year, the first solar power plant for irrigation pumping was erected at Al Maadi, Egypt (Duffie and Beckman, 1991; Raafat, 1994). In the 1980s, nine Solar Electric Generating Systems (SEGSs) were erected in the California desert, more than a century later. Then, years later, parabolic trough technology was integrated into the fossil fuel combined cycle to boost solar energy conversion. The Integrated Solar Combined Cycle (ISCC) is created by combining a solar field with a combined cycle.Allani et al. were the first to do an ISCC analysis in Tunisia (1997). The ISCC is more profitable than SEGS, according to the authors. Dersch et al. (2004) compared the performance of the ISCC to SEGS and Combined Cycle (CC) power plants using Gate Cycle and IPSEpro. They've come to the conclusion that the ISCC is the most effective. Kane and Favrat (1999) focused on the ISCC's heat exchangers. They demonstrated that the ISCC with twofold pressure-reheat and a smaller solar field outperforms the competition.

Manente (2016) offered a novel ISCC side-by-side off-design model of a 390 MWe in a recent study. Thermoflex software was utilized by the author to create an accurate model. Rovira et al. (2016) compared the annual performance and economic feasibility of Integrated Solar Combined Cycles using two solar concentration technologies: parabolic trough collectors (PTC) and linear Fresnel reflectors (LFR) (ISCC). According to the authors, using Fresnel technology in ISCC is one of the most promising economic results when both optimistic and cautious scenarios are evaluated.

The investigation of the ISCC performance in India has piqued the curiosity of numerous researchers. In this study, the authors chose the Hassi R'mel in the southern of Algeria. Aside from Hassi R'mel, numerous other Algerian localities are being explored for solar thermal power plants in the near future. The current research examines the thermal performance of an ISCC in a tropical climate at Kalburgi, Karnataka, India. To estimate the direct solar irradiance intensity, an accurate model with seven alternative ways of tracking has been constructed.A simple model has been proposed in this study to assess the direct component of solar irradiation in the Algerian climate. The total hourly, daily, and monthly direct radiation incident on seven different oriented solar concentrators was estimated using just the monthly mean daily global and diffuse horizontal sun irradiance data for Tamanrasset, Algeria.

The seven different tracking systems are shown in below.
C1: A fixed surface south facing (Besarati et al., 2013),
C2: A surface rotated about a horizontal north–south axis

(Goswami et al., 2000),
C3: A surface rotated about a horizontal east–west axis
(Goswami et al., 2000),
C4: A surface oriented at an angle γ with the south, with a tilt
angle of 45◦
(El Mghouchi et al., 2014)),
C5: A surface tilted at the latitude angle with East–West tracking (Besarati et al., 2013),
C6: A surface tilted at the latitude angle with azimuth tracking
(Goswami et al., 2000),
C7: A surface oriented with azimuth/elevation tracking axis
(Goswami et al., 2000),

The declination angles s, which represent the monthly mean hourly direct sun irradiation intercepted by the concentrator aperture, were computed using the following standard relationships:

The day of the year The day of the year nj is calculated taking into account the hour of the day; it can be calculated by the formula: nj = n0 + 1 24 · (h + min 60 + s 3600). (1) This formula gives time in seconds.

Declination and sunrise hour angles

The declination (δs) and the sunrise hour angles (ωs) are defined by the following equations (Duffie and Beckman, 1991): δs = 23.45◦ sin (360(284 + nj) 365) (2) ωs = arcos(− tan ϕ · tan δs).

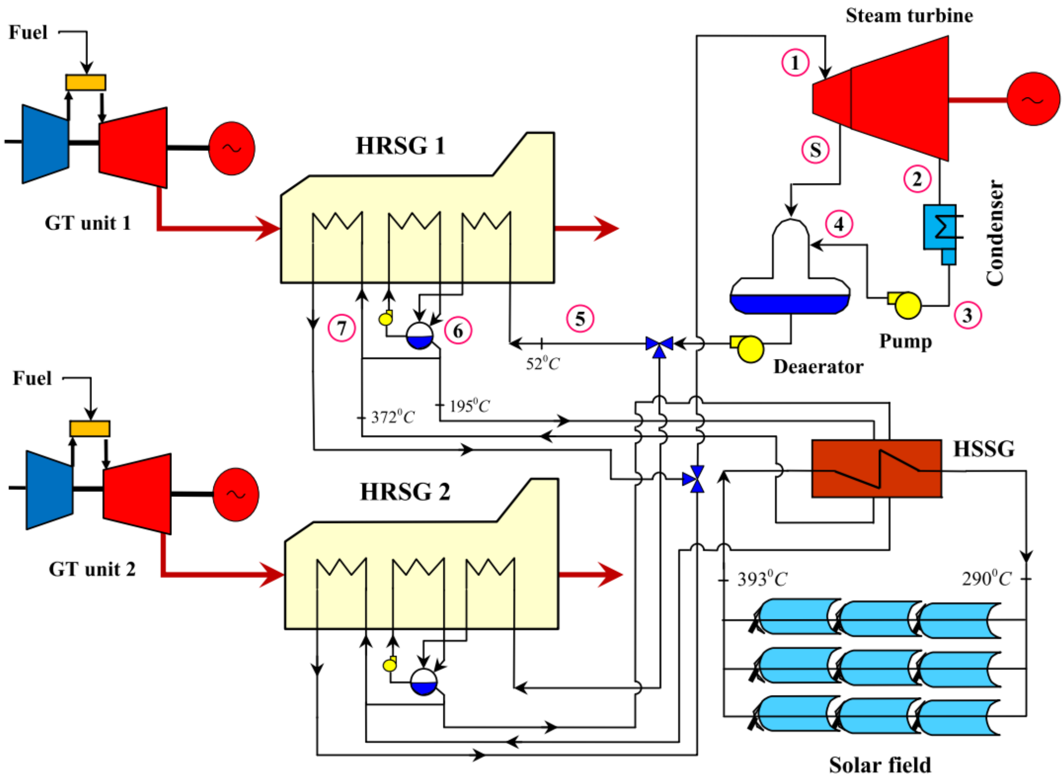

Fig.1 Typical Integrated solar combined cycle

Throughout the year, the data in Fig. 3 show that the collector with two axis tracking (case 7) gains the greatest energy compared to the other collection tracking methods. In summer, the direct solar irradiation provided by the horizontal N–S axis, polar N–S tracking, and tilted tracking axis aperture to the south per latitude local (cases 3, 5 and 6) is superior to the horizontal E–W axis tracking and a tilted surface at an angle of 45 (cases 2 and 4), and in winter, the horizontal E–W axis tracking is higher than the horizontal N–S. The fixed aperture to the south, on the other hand, is the least efficient of all the designs.

As shown in the fig 2,We can see that the monthly mean direct solar irradiation for (case 7) fluctuates between 7 and 9 kWh/m2 day; however, the direct solar irradiation potential for cases (2, 3, 4, 5 and 6) is between 5 and 8 kWh/m2day, and between 4 and 6 kWh/2day in the case (1). According to the current study, Tamanrasset has more radiation than the rest of Algeria, and so presents a promising opportunity to install solar thermal power projects that have been mentioned in Algeria's renewable energy programme. A comprehensive thermal performance of an ISCC under Tamanrasset climate is shown in the following sections to highlight the benefits of installing a solar.In the next sections, a detailed thermal performance of an ISCC in Tamanrasset climate is shown to emphasize the benefits of installing a solar thermal power plant.

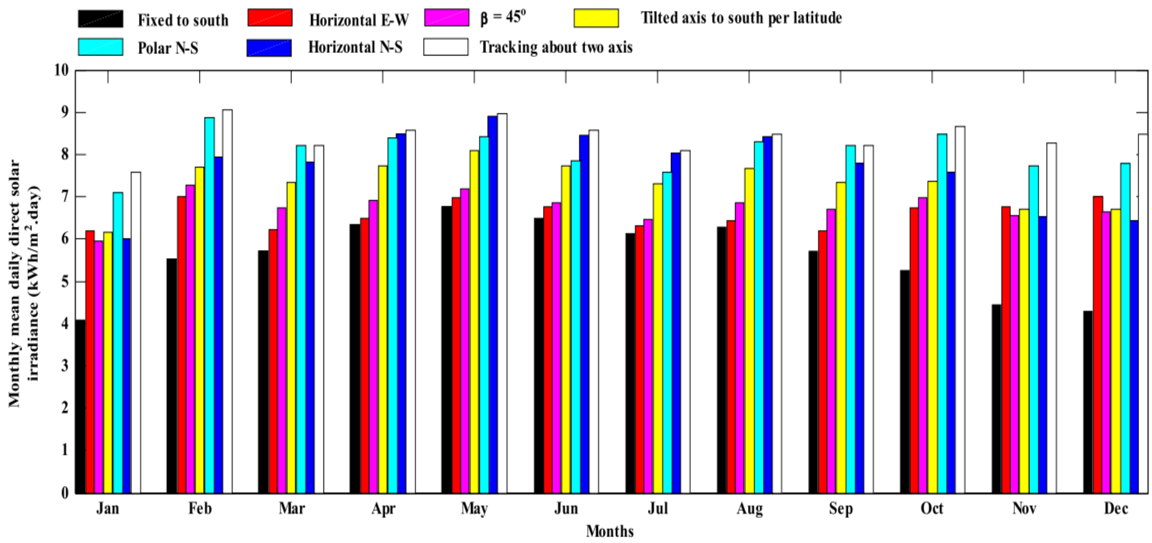

Fig.2 Monthly mean direct solar radiation

1.1Description of power plant components

A parabolic trough solar field plus a fossil fuel combined cycle make up a typical Integrated Solar Combined Cycle (ISCC). The ISCC proposed in this study is similar to the one that is currently in use at Hassi R'mel. The plant's combined cycle consists of two gas turbines and an enormous steam turbine to give a wide range of operation. Hundreds of parabolic trough collectors make up the solar field.

1.1.1 Parabolic trough collectors

Reflector, receiver, tracking system, and a metal structure make up a conventional parabolic trough collector. The reflector is constructed out of high-reflectivity mirrors. The receiver is a black metal tube that is placed on the focal line of the concentrator and packed in a glass tube to reduce heat loss due to convection. To enhance solar energy collection, the axis of rotation of the parabolic trough collector in this study is directed north–south.

1.1.2 Solar field

The suggested integrated solar combined cycle, as shown in Fig. 1, is made up of the following components: a solar field, two gas turbine units, and a steam turbine. The solar field is the most important portion of the plant. It is made up of 56 loops, each with six collectors organized in parallel rows (type of LS-3). The collectors have single axis tracking, with the north–south axis aligned, so they track the sun from east to west. In this study, the Therminol VP-1 heat transfer fluid was chosen.

The proposed scheme's power plant is a typical combined cycle power plant with two 40 MWe gas turbine units (type SGT800) and an 80 MWe steam turbine (type SST-900). A solar steam generator is connected to two identical single-pressure heat recovery steam generators (HRSG). Thermal energy from the solar field is combined with the heat of the gas turbine exhaust gases during sunny periods.Two Brayton cycles are coupled to a single pressure level Rankine cycle via a heat recovery steam generator in the plant diagram shown in Fig. 2. (HRSG). This is connected to a solar steam generator in parallel (Derbal-Mokrane et al., 2012).

1.2 Thermodynamic modeling of the ISCC

1.2.1 Modeling of solar field

To size the solar field, a model was created. The chosen location is ‘‘Kalburgi" city, as indicated above. The following are the geographical parameters of this location: 17.758, 76.3676 longitude, and 750m altitude.
Date: time (day of the year, hour).
• Geographic coordinates (latitude and longitude).
• Geometric design: (Dimensions of the solar field).
• Optics: (absorption and transmission coefficients of collector components).
The amount of solar energy collected is determined by the collector's optical performance and the angle of incidence between the solar beam and the direct sun reflector's surface (Badescu, 2002) The thermal power of a

parabolic trough collector, on the other hand, is affected by the collector's heat losses. As a result, the collector Qu's usable energy can be stated as:

$\dot{Q}\ abs = Ac \cdot DNI \cdot \eta$

$\dot{Q}\ c = \dot{Q}\ abs - \dot{Q}\ HeatLoss$

1.2.2 Modeling of the ISCC

Solar combined cycle with integrated solar power ISCC power plants use waste heat to generate electricity via a gas turbine and a solar steam generator to produce steam, which is then used to generate further energy via a steam turbine. The Gas turbine cycle and Steam turbine cycle equations, as found in Boyce, are excellent for estimating ISCC power plants (2002)

1.2.3 Modeling of Gas turbine

The difference between the real compressor work WC and the actual turbine work WG is the network of the gas turbine WGT. Ibrahim et al. (2011) provided the following formulas for calculating the turbine and compressor work:

1.2.4 Modeling of steam turbine

According to the mathematical model listed below, the steam Rankine cycle has been performed using mass and energy conservation equations (Safarian and Aramoun, 2015).

Firstly, we use heat balance around the Deaerator (Fig. 1) to find Y: $Y = h5 - h4\ hS - h4$.

Secondly, the air to steam ratio is found from heat balance around the heat exchanger: $\dot{m}\ a\ \dot{m}\ steam = h5 - h1\ Cpa(T4' - T1')$

where the network of steam turbine is:

$WST = \dot{m}\ steam \cdot [Y \cdot (h1 - hS) + (1 - Y)(h1 - h2)]$. (40)

The heat required from the condenser is calculated as:

$QC = \dot{m}\ steam \cdot (1 - Y)(h3 - h2)$. (41)

The feed water pump work is:

$WFP = \dot{m}\ steam \cdot (h4 - h3)$.

We used the international tables of water properties (saturated area and superheated steam region) from the reference (engel et al., 2015) to compute inlet/outlet the enthalpy and pressure of steam in the most essential sites of the Rankine water–steam cycle, as shown in Fig. 2.

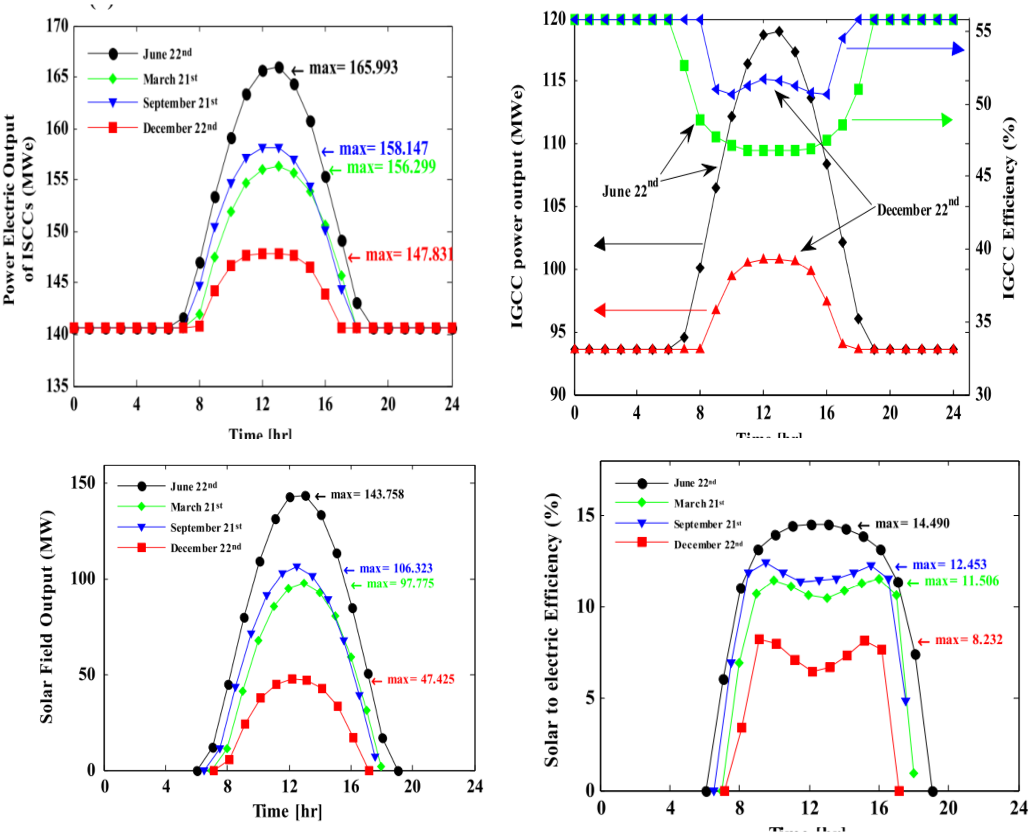

II. Discussion Of The Results

Based on the aforesaid modelling, a thermodynamic model has been built. This comprises solar radiation, the solar field, and power conversion cycles modelling. Because the solar field's efficiency has such a big impact on the ISCC's performance, it's crucial to look at it. We can deduct from Fig. 1 that the solar field's efficiency could reach 77.48 percent in the summer. In the winter, though, it might be as low as 48.08 percent. The solar field efficiency can reach 69.91 percent in the spring and 65.84 percent in the autumn.

Because the solar field operates on a variable flow approach, the HTF's input and outlet temperatures are kept constant. The intake and output HTF temperatures in the field for this investigation are 290°C and 393°C, respectively. Figure 2 depicts the fluctuation in HTF mass flow. It is self-evident that the more the solar radiation, the higher the HTF's mass flow rate. As solar radiation rises, so does absorbed solar energy, resulting in an increase in solar field thermal energy gain.

We have carefully examined the ISCC's performance over the course of a year. In terms of the power plant's overall performance, the total energy production, as shown in Fig.2, could achieve a maximum of 155 MW in the first period and a minimum of 131 MW during low radiation times. The ISCC is in boosting mode, which means that the more solar radiation there is, the more electricity the power plant produces. This is owing to the heat recovery steam generator's increased steam mass flow (HRSG). The ISCC's overall efficiency is a significant element.

Solar to electricity efficiency in four seasons is simulated to illustrate the effectiveness of converting solar energy. During the winter, even when the DNI is at its highest, the solar to power efficiency declines at noon. This is due to the angle of incidence of the sun. During the summer, however, solar to electricity conversion efficiency can reach 14.490 percent (Fig. 6(d)). As indicated in Fig. 8(a), the overall steam turbine output at the design point is 69 MW, which represents a 23 MW increase in power generation compared to 47 MW at night, while the steam turbine efficiency is 53% in summer and 51% in winter at the design point, and 50% at night.

References

[1]. Collares-Pereira, M., Rabl, A., 1979. The average distribution of solar radiationcorrelations between diffuse and hemispherical and between daily and hourly insolation values. Sol. Energy 22, 155–164.

[2]. Derbal-Mokrane, H., Bouaichaoui, S., Gharbi, N.E., Belhamel, M., Benzaoui, A., 2012.Modeling and numerical simulation of an Integrated Solar Combined Cycle System in Algeria. Procedia Eng. 33, 199–208.

[3]. Dersch, J., Geyer, M., Herrmann, U., Jones, S.A., Kelly, B., Kistner, R., Ortmanns, W.,Pitz-Paal, R., Price, H., 2004. Trough integration into power plants — a study on the performance and economy of integrated solar combined cycle systems. Energy 29, 947–959.

[4]. Duffie, J.A., Beckman, W.A., 1991. Solar Engineering of Thermal Processes. J. Wiley.El Mghouchi, Y., El Bouardi, A., Choulli, Z., Ajzoul, T., 2014. New model to estimate and evaluate the solar radiation. Int. J. Sustain. Built Environ. 3, 225–234.Emun, F., Gadalla, M., Majozi, T., Boer, D., 2010. Integrated gasification combined cycle (IGCC) process simulation and optimization. Comput. Chem. Eng. 34, 331–338.

[5]. Franchini, G., Perdichizzi, A., Ravelli, S., Barigozzi, G., 2013. A comparative study between parabolic trough and solar tower technologies in Solar Rankine Cycle and Integrated Solar Combined Cycle plants. Sol. Energy Part C 98, 302–314.Goswami, D.Y., Kreith, F., Kreider, J.F., Kreith, F., 2000. Principles of Solar Engineering. Taylor & Francis, Philadelphia, PA.L. Achour et al. / Energy Reports 4 (2018) 207–217 217

[6]. Gülen, S.C., 2015. Second law analysis of integrated solar combined cycle power plants. J. Eng. Gas Turbines Power 137, 051701. Ibrahim, T.K., Rahman, M.M., Abdalla, A.N., 2011. Gas turbine configuration for improving the performance of combined cycle power plant. Procedia Eng. 15, 4216–4223.

[7]. Kane, M., Favrat, D., 1999. Approche de conception et d'optimisation de centralesolaire intégrée à cycle combinéinspirée de la méthode du pincement (partie II: réseau d'échangeurs de chaleur). Int. J. Therm. Sci. 38, 512–524.

[8]. Khaldi, F., 2012. Energy and exergy analysis of the first hybrid solar-gas power plant in Algeria. In: ECOS. pp. 26–29.

[9]. Li, Y., Yang, Y., 2014. Thermodynamic analysis of a novel integrated solar combined cycle. Appl. Energy 122, 133–142.

[10]. Li, Y., Yang, Y., 2015. Impacts of solar multiples on the performance of integrated solar combined cycle systems with two direct steam generation fields. Appl. Energy 160, 673–680.

[11]. Rovira, A., Barbero, R., Montes, M.J., Abbas, R., Varela, F., 2016. Analysis and comparison of Integrated Solar Combined Cycles using parabolic troughs and linear Fresnel reflectors as concentrating systems. Appl. Energy 162, 990–1000.

Pavankumar Deshmukh. "Performance analysis of Integrated solar combined cycle in the southern state of India." *IOSR Journal of Mechanical and Civil Engineering (IOSR-JMCE)*, 18(5), 2021, pp. 17-21.